Articles

Pt(II) Complexes of a Combretastatin A-4 Analogous Chalcone: Effects of Conjugation on Cytotoxicity, Tumor Specificity, and Long-Term Tumor Growth Suppression

Rainer Schobert,*,† Bernhard Biersack,† Andrea Dietrich,§ Sebastian Knauer,† Miroslava Zoldakova,† Angelika Fruehauf,§ and Thomas Mueller§

Organic Chemistry Laboratory, University of Bayreuth, Universitätsstrasse 30, 95440 Bayreuth, Germany, and Department of Internal Medicine IV, Oncology/Hematology, Research Laboratory, Martin Luther University Halle-Wittenberg, 06099 Halle, Germany

Received August 7, 2008

Three dichlorido(6-aminomethylnicotinate)platinum complexes **6** comprising a combretastatin A-4 analogous chalcone were tested on a panel of 21 tumor cell lines from 9 entities. Parent chalcone **1a** and the directly linked conjugate **6a** exhibited excellent antiproliferative activities, similar in magnitude [average log(IC_{50}) values of −7.3 (**1a**) and −7.0 (**6a**)] and cell line specificity but slightly different in the mechanism of apoptosis induction. While **1a** and **6a** caused an equally fast rise in caspase-9 in the tested cancer cell lines, the downstream effector caspase-3 built up faster in cells treated with **1a** compared to **6a**, yet reached an equal end level. They also had different long-term effects on the regrowth of cancer cells treated with a single dose. In contrast, conjugates **6b**,**c** featuring longer spacers between the Pt complex and the chalcone moieties were less antiproliferative than **6a**.

Introduction

The anticancer agent combretastatin A-4 (Figure 1), a naturally occurring *cis*-stilbene from the bark of the South African Cape Bushwillow (*Combretum caffrum*), binds to the colchicine binding site of β-tubulin and interferes with the polymerization of tubulin. Its water soluble phosphate ester has already entered clinical phase III trials. Combretastatin A-4 is strongly angiotoxic and also active in MDR[a] positive tumors.[1] Since the thermodynamically favored trans isomer of combretastatin A-4 is much less active, a search for chemically more stable active analogues began that eventually led to the methoxy functionalized chalcones **1a** and **1b**. Both showed high activity in K562 leukemia cells.[2] The biological potential of chalcones is amazing because of their tubulin binding and alkylating properties and their possible interactions with various proteins related to cell apoptosis and proliferation. However, systematic studies of chalcones have only started to emerge.[3−6] Some chalcones were found to increase the level of the tumor suppressor protein p53 in various cancer cell lines by disrupting its complexes with the oncoprotein MDM2.[3] Simple structure−activity studies were undertaken in order to optimize the antiproliferative efficacy of libraries of synthetic chalcones in HT-29 colon cancer cells where the best performers reached IC_{50} values below 10 μM.[4] Heteroaryl substituted chalcones were developed as inhibitors of vascular cell adhesion molecule-1 (VCAM-1) expression for the treatment of chronic inflammatory diseases.[5]

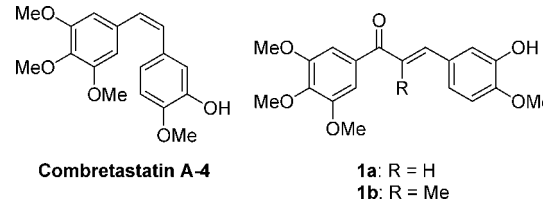

Figure 1. Combretastatin A-4 and chalcone analogues **1a**,**b**: potent inhibitors of tubulin polymerization.

But hitherto, apart from N-mustards and DNA minor groove binding pyrrolo[2,1-*c*][1,4]benzodiazepines,[7] no conjugates have been disclosed of combretastatin A-4 or related chalcones with clinically established anticancer drugs that operate by a different mode of action such as DNA-targeting platinum(II) complexes. We now prepared such conjugates of chalcone **1a** by our protocol based upon the esterification of 6-aminomethylnicotinate ligands.[8−11] The product chalcone−Pt(II) complex conjugates **6** were tested on a representative panel of 21 tumor cell lines and nonmalignant fibroblasts. Their efficacy, specificity, regrowth retardation, and mechanism of induction of apoptosis were compared with those of free parent chalcone **1a** in order to pinpoint beneficial synergisms of conjugating DNA-seeking platinum and tubulin-targeting chalcone moieties.

Results and Discussion

Chemistry. Chalcone **1a** was prepared from isovanillin and 3,4,5-trimethoxyacetophenone in one step according to a modified literature procedure.[2] The hydroxyalkyl functionalized chalcones **3** were synthesized via Williamson etherification of the chalcone **1a** with tetrahydropyranyloxyalkyl bromide in the presence of K_2CO_3 and tetrabutylammonium iodide (TBAI) followed by deprotection of the intermediate THP ethers **2** with PPTS in ethanol (Scheme 1). Boc-protected 6-aminomethylnicotinic acid[8] was connected to the chalcones **1a** and **3** by

* To whom correspondence should be addressed. Phone: +49(0)921 552679. Fax: +49(0)921 552671. E-mail: Rainer.Schobert@uni-bayreuth.de.
† University of Bayreuth.
§ Martin Luther University Halle-Wittenberg.

[a] Abbreviations: DIABLO, direct IAP-binding protein with low isoelectric point; DMAP, 4-dimethylaminopyridine; IAP, inhibitor of apoptosis protein; MDR, multidrug resistance; PARP, poly(ADP-ribose) polymerase; PPTS, pyridinium *p*-toluenesulfonate; Smac, second mitochondria-derived activator of caspase; SRB, sulforhodamine-B; TBAI, tetrabutylammonium iodide; TUNEL, terminal deoxynucleotidyl transferase-mediated dUTP nick-end labeling.

10.1021/jm801001d CCC: $40.75
Published on Web 12/22/2008

Scheme 1. Synthesis of Chalcone−Platinum(II) Complex Conjugates **6**[a]

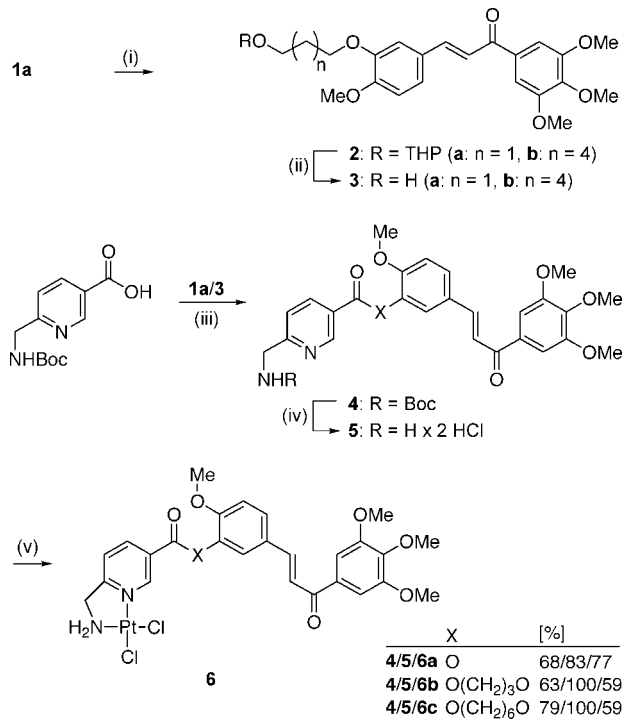

[a] Reagents and conditions: (i) K_2CO_3, THP-alkyl bromide, TBAI, DMF, 24 h, room temp, 95−99%; (ii) PPTS, ethanol, 1 h, reflux, 81−84%; (iii) Et_3N, $C_6H_2Cl_3COCl$, DMAP, alcohol **1a** or **3**, DMF/toluene (1:10), 16 h, room temp; (iv) 4 M HCl/dioxane, 1 h, room temp; (v) K_2PtCl_4, aqueous THF, pH 5−6, 24 h, room temp.

Yamaguchi esterification to give the respective esters **4**.[8,9] Deprotection of the amino group in HCl/dioxane and treatment of the resulting ammonium chlorides **5** with K_2PtCl_4 in aqueous THF under slightly acidic conditions (pH 5−6) gave the Pt(II) complexes **6**.[8−11]

Biological Evaluation. Chalcone **1a** and the directly linked conjugate **6a** showed a similar spectrum of antiproliferative activity (Table 1) and specificity (Figure 2) in the tested cell lines. Chalcone **1a** was generally more active than the platinum conjugate **6a**. This corroborated the assumption that compounds **6** might act as intact conjugates within the cells. However, while they proved stable in PBS at 37 °C for more than 96 h, we cannot exclude their intracellular enzymatic hydrolysis. The observed activities of **1a** and **6a** were extraordinary by any standard even in cell lines insensitive or refractory to cisplatin (H322, H358, SW1736, 8505C, DLD-1) or to 5-fluorouracil and/or oxaliplatin (DLD-1, SW480) (data not shown). The log(IC_{50}/96 h) values averaged over all 21 cell lines were −7.3 (**1a**) and −7.0 (**6a**); i.e., IC_{50} values lay mostly in the double-digit nanomolar range. The similarities in their activity profiles speak for the two compounds probably acting on the same targets in most cell lines. This would also be in line with data recently published by Tron et al., who investigated combretastatin A-4 conjugates with various N-mustards.[12] They found a generally high activity with combretastatin A-4 being more potent than the corresponding chlorambucil ester except for one particularly sensitive neuroblastoma cell line (SH-SY5Y) in which the conjugate showed enhanced potency. The cell line most susceptible to compounds **1a** and **6a** (IC_{50}/96 h ≈ 20 nM) was the cervical carcinoma cell line A431, whereas HT-29 colon carcinoma cells and breast tumor BT474 cells were least sensitive.

Table 1. Inhibitory Concentrations IC_{50} (nM)[a] for Compounds **1a** and **6a−c**

cell panel	cell line	**1a**	**6a**	**6b**	**6c**
germ cell	H12.1	33.6 ± 13	61.6 ± 12		4200
	2102EP	31.4 ± 5	49.0 ± 3	11000	4400
	1411HP	141.8 ± 41	283.2 ± 90	14000	5300
colon	HCT-8	56.0 ± 10	167.0 ± 20	11000	3300
	HCT-116	25.1 ± 4	61.7 ± 9	12000	4800
	HT-29	2600 ± 500	>10000	21000	5300
	DLD-1	32.3 ± 2.8	62.0 ± 10	13000	5000
	SW480	102 ± 35	93 ± 106	11000	8400
non-small-cell lung	A549	67.5 ± 14	132.4 ± 32	14000	
	A427	51.2 ± 14	92 ± 68	12000	4400
	H322	39.0 ± 2	58.0 ± 7	11000	
	H358	17.1 ± 2	26.2 ± 6	7100	
head-and-neck	FADU	41.0 ± 11	57.6 ± 7	4300	6000
	A253	22.8 ± 3	49.7 ± 8	13500	
cervix	A431	15.0 ± 3	24.7 ± 2	6300	3000
mamma	MCF-7	22.3 ± 12	144.1 ± 60	8800	4000
	BT474	193.2 ± 38	8500 ± 2300	18000	7000
ovarian	A2780	15.6 ± 3	28.7 ± 5	10500	4200
melanoma	518A2	33.6 ± 3	57.2 ± 11	14000	5000
thyroidal	8505C	49.7 ± 3	88.1 ± 19	17000	5500
	SW1736	27.5 ± 4	53.4 ± 10	16000	5700

[a] Values are derived from dose−response curves obtained by measuring the percentage of surviving cells relative to untreated controls after 96 h of exposure of cells to test compounds using the SRB assay. Values for **1a** and **6a** represent mean values from three independent experiments. Values for **6b** and **6c** are the average of two experiments.

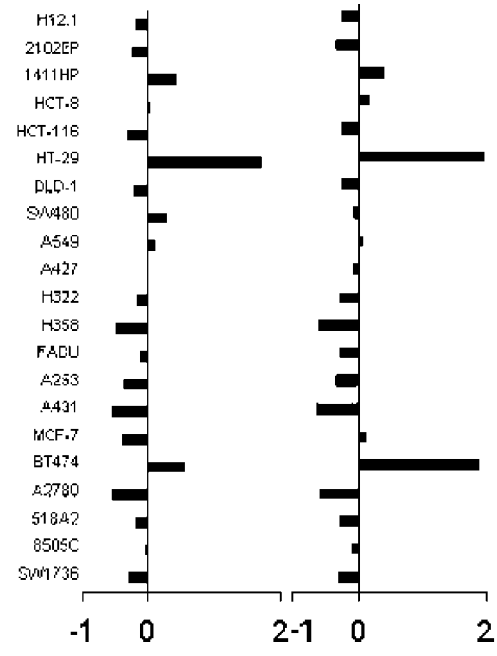

Figure 2. Cell line specificities of chalcone **1a** (left) and Pt conjugate **6a** (right) as deviation of the log(IC_{50}/96 h) of individual cell lines from the mean over all cell line log(IC_{50}/96 h) values. Negative values indicate higher and positive values lower than average activities. Mean log(IC_{50}/96 h) values are −7.3 (**1a**) and −7.0 (**6a**).

Increasing the distance between platinum complex and chalcone moieties by introducing a spacer had a dramatic effect on the cytotoxicity (Table 1) and to some extent also on the cell line specificity profile, possibly by curtailing some synergetic modes of action or by addressing other cellular targets or by leading to differerent hydrolysis products with divergent activities. The alkyl spacered conjugates **6b** and **6c** had up to 1000 times greater IC_{50} values than complex **6a**. The hexyl-tethered conjugate **6c** proved generally more active than the

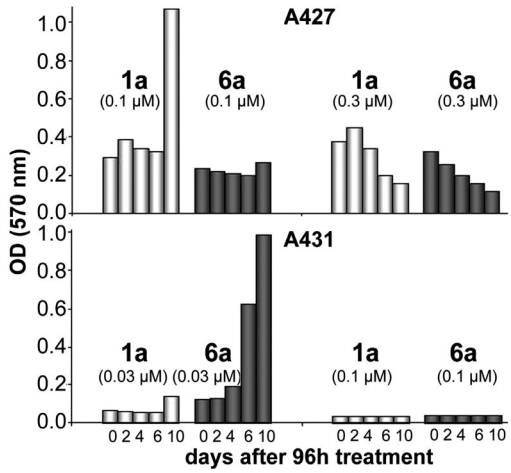

Figure 3. Regrowth of cell cultures of A427 non-small-cell lung cancer cell line (top) and A431 cervical cancer cell line (bottom) over a 10-day period following treatment with **1a** or **6a** at the indicated concentrations for 96 h. Data are representatitive of three independent experiments.

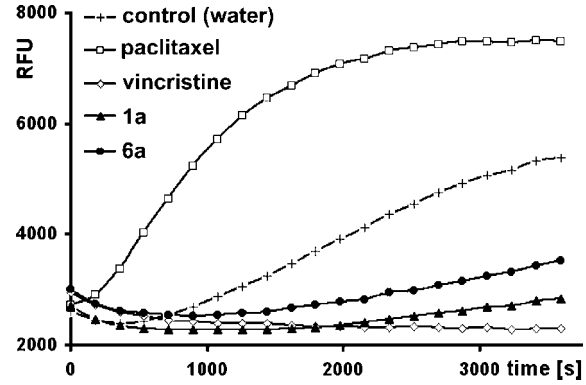

Figure 4. Effects of 3 μM each of compounds **1a**, **6a**, vincristine, and paclitaxel on the polymerization of tubulin as ascertained with a fluorescence-based assay kit from Cytoskeleton. Data are representative of three independent experiments. RFU = relative fluorescence units.

propyl-linked **6b** (except for FaDu human head-and-neck squamous cell carcinoma cells).

Beside low IC_{50} values, other qualities of potential new anticancer drug candidates matter as well, such as their ability to suppress a regrowth of cancer cells following a single-dose impact. Tron et al. reported that combretastatin A-4 and its chlorambucil ester were unable to kill all cells of SH-SY5Y neuroblastoma cultures even at high concentrations despite their relatively low IC_{50} values. A significant cell viability of ~10% persisted.[12] We observed a similar behavior of the chalcones **1a** and **6a** for certain cell lines. While the dose−response curves of sensitive cell lines such as A431, A2780, HCT-116, and DLD-1 crossed the IC_{90} threshold (10−100 nM) early on, those of the less sensitive 1411HP, BT474, SW480, and HT-29 cells leveled off considerably toward higher concentrations. For 5 tumor cell lines out of the panel of 21 we also observed distinct differences in the long term regrowth retardation by chalcone **1a** and its conjugate **6a**. These tumor cell lines were treated once with drug concentrations around the IC_{90} values for 96 h and then were rinsed drug-free and resuspended with fresh media. Their regrowth was monitored over the following 10 days. A one-off treatment with 0.1 μM conjugate **6a** prevented regrowth of A427 non-small-cell lung cancer cells and cisplatin-resistant 1411HP germ cell tumor cells more effectively than a comparable exposure to the free chalcone **1a**, while the latter performed better at low concentrations in eradicating A253 head-and-neck carcinoma cells, A431 cervical carcinoma cells, and A2780 ovarian carcinoma cells. The growth kinetics of treated cells of A427 and A431 are depicted in Figure 3. There are several plausible explanations for these divergent long-term effects such as a shift in targets, or differences in cellular storage or induction of resistance. Alternatively, cleavage of **6a** in cells of A427 to give **1a** and auxiliary platinum complexes could be responsible for its superior effect, while in cells of A431 either such cleavage occurs to a lesser extent or the mixture of cleavage products is less efficacious for unknown reasons.

Next we addressed the effects of compounds **1a** and **6** on the potential targets DNA and tubulin. When the compounds were incubated at concentrations of 5−60 μM with pBR322 plasmid DNA, no effect on the electrophoretic mobilities of the various morphologically different DNA forms present was visible. This means the tested compounds at relatively low concentrations either do not bind to plasmid DNA or upon binding do not change the DNA morphology. Then the metal content of salmon sperm DNA treated with high doses (100 μM) of platinum complexes **6a** and **6c** was quantified by inductive coupled plasma optical emission spectroscopy (ICP-OES). This method furnished Pt content in the DNA samples of 0.05% for **6a** and 0.037% for **6c**, which is about 4 times less than the 0.187% we found for the good DNA-binder cisplatin.

Compounds **1a** and also **6a** to a lesser extent inhibited the polymerization of tubulin when applied in vitro at physiologically meaningful concentrations of 3 μM using the tubulin polymerization assay kit by Cytoskeleton. Figure 4 shows the time dependency of this process in samples containing **1a**, **6a**, or the reference compounds paclitaxel, a known accelerator, or vincristine, a known inhibitor of microtubule formation. The differences in the tubulin polymerization rates of **1a** and **6a** roughly correlate with their average antiproliferative effects in tumor cells.

Compounds **1a** and **6a** are inducers of apoptosis in cancer cells, detectable in its late stages by means of the TUNEL assay that labels the 3′-OH ends of typical DNA fragments with fluorescein-tagged nucleotides.[13] It was conducted employing the in situ cell death detection kit (Roche) with HL-60 leukemia and 518A2 melanoma cells that had been exposed to 10 μM concentrations of compounds **1a** and **6a** for 15 h. Fluorescence microscopy revealed apoptotic cells as green fluorescent spots that were counted and compared with the overall cell numbers. At the end of the exposure period about 50−60% of the 518A2 cells and about 40−50% of the HL-60 cells were apoptotic.

To determine whether apoptosis was initiated by compounds **1a** and **6a** via the same mechanism, we carried out immunoblotting assays for caspase-9, a central enzyme in the intrinsic mitochondrial apoptosis pathway, as well as for the downstream effector caspase-3 and for the PARP protein which plays a pivotal role in the nucleotide excision repair (NER) of DNA lesions and which is cleaved during apoptosis. Figure 5 shows Western blots for caspase-9 in HL-60 leukemia cells pre-exposed to the compounds and then lysed after 0−30 h periods. The cell protein was separated by electrophoresis, blotted onto PVDF, treated with antibodies against caspase-9, and visualized. Both compounds gave a congruent time-dependent profile of procaspase-9 and cleaved/activated caspase-9 concentrations with a maximum of the latter after ~7 h past exposure, indicating an activated mitochondrial apoptosis.

Next, A2780 ovarian cancer cells, 518A2 melanoma cells, and DLD-1 colon carcinoma cells as well as nonmalignant

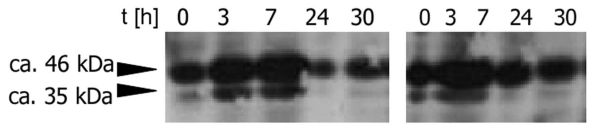

Figure 5. Time-dependent processing of procaspase-9 (~46 kDa) to activated caspase-9 (~35 kDa) in HL-60 leukemia cells treated with 10 μM compounds **1a** (left) and **6a** (right) for 0, 3, 7, 24, and 30 h. Shown is ECL-visualization of lysates immunoblotted with prim./sec. antibodies to caspase-9 from Calbiochem. Data are representative of three independent experiments.

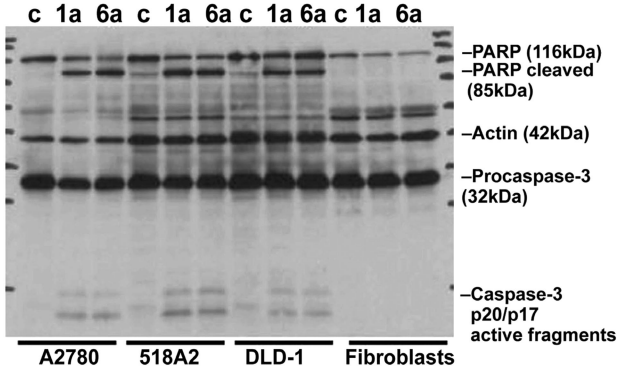

Figure 6. Western blots for analysis of cleavage/activation of caspase-3, cleavage of PARP and actin as loading control in A2780 ovarian cancer cells, 518A2 melanoma cells, DLD-1 colon cancer cells, and nonmalignant human WW070327 fibroblasts after a 24 h treatment with 1 μM **1a** or 1 μM **6a**; c means untreated control cells. Data are representative of three independent experiments.

human fibroblasts WW070327 were treated for 24 h with 1 μM concentrations of **1a** and **6a**, which amounts to 30−60 times the IC_{50} in the case of the tested cancer cell lines. Then the cell samples were analyzed by Western blotting for cleavage/activation of caspase-3 and for cleavage of PARP. The cytoskeleton component actin was used as a loading control. Figure 6 shows that there was virtually no difference in apoptosis induction of the three cancer cell lines treated with either **1a** or **6a**. Both compounds caused a significant increase of the activated form of caspase-3 and of the cleaved form of PARP relative to an untreated control (C). This is typical of an apoptotic cell death. In contrast, the nonmalignant fibroblasts showed no signs of apoptosis when treated with the same 1 μM doses of **1a** or **6a**. This is a pharmacologically promising aspect.

We also monitored the progress of the caspase-3 rise in the hours immediately following the exposure of HL-60 leukemia cells to compounds **1a** and **6a** by means of the colorimetric CASPASE-3 cellular activity assay kit PLUS from Biomol. The cells were lysed, and caspase-3 activity was measured with a specific dye-labeled substrate, i.e., Ac-DEVD-(*p*-nitroanilide). The initial rate of the cleavage of this substrate was ascertained by measuring the extinction of the samples, which was taken as equivalent to the respective concentration of caspase-3. Interestingly, levels of caspase-3 in cells treated with the two compounds were comparable only from 15 h exposure time on (Figure 7). Until then, the caspase-3 concentration grew more slowly in cells exposed to the conjugate **6a** when compared to **1a**. Some biosynthetically close relatives of **1a** such as curcumin, resveratrol, and quercetin are known to sensitize cancer cells to proapoptotic stimuli by inducing proteins that negatively regulate apoptosis-inhibiting proteins (IAP).[14−16]Some members of the IAP family, such as survivin, block apoptosis by specifically

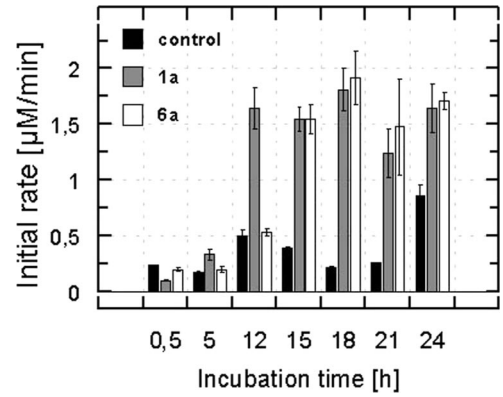

Figure 7. Initial rates of cleavage of substrate Ac-DEVD-(*p*-nitroanilide) by caspase-3 isolated from HL-60 leukemia cells treated with 1 μM **1a** or **6a** or a control (C) for the indicated times, calculated from the initial slope of the absorbance vs time curves. Data represent the mean values of three experiments.

binding to and inhibiting caspase-3 but not the initiator caspase-9.[17] Possibly, chalcone **1a** caused a faster release than conjugate **6a** of IAP-inactivating proteins, such as Smac/DIABLO. This is remarkable, as platinum drugs were themselves reported to decrease IAP levels and to induce apoptosis in sensitive cancer cells.[18]

Conclusions

The chalcone−platinum complex conjugate **6a** exhibited excellent tumor growth inhibition across a panel of 21 cell lines, similar in magnitude and cell line specificity to the activity of the free chalcone **1a**. However, cell line specific differences were found in the long term effect of **1a** and **6a** on the regrowth of cancer cells treated with a single dose. At low 0.1 μM concentration, **6a** prevented regrowth of A427 non-small-cell lung cancer cells and 1411HP germ cell tumor cells more effectively than **1a** while the latter performed better in eradicating A253 head-and-neck carcinoma cells, A431 cervical carcinoma cells, and A2780 ovarian cancer cells at very low 0.03 μM concentrations. Whether a shift to other cellular targets or the combined effect of conceivable hydrolysis products of **6a** plays a role here remains unclear. In preliminary in vitro experiments, the Pt complexes **6** interacted with various forms of DNA, though less tightly than cisplatin, achieving significant metalation only at superclinical concentrations. Tubulin seemed to be the primary target of both compounds **1a** and **6a**, which at different rates inhibited its polymerization in vitro at physiologically meaningful concentrations. These rate differences would match the different cytotoxicity profiles of **1a** and **6a** and yet cannot explain the subtle differences in cell line specific regrowth retardations and in caspase kinetics. The mode of cell death initiated by chalcones **1a** and **6a** in cells of various cancer cell lines was predominantly apoptotic as indicated by the activation of caspases-9 and -3, by cleavage of PARP, and by TUNEL. We found a slower progression from caspase-9 to caspase-3 in cancer cells treated with **6a** compared to those treated with **1a**. This could be due to an intracellular cleavage of **6a** to give the more active **1a** and platinum complexes or to a slower release of proapaptotic proteins such as Smac/DIABLO from the mitochondria exposed to **6a** when compared to **1a**. A series of immunoblotting kinetics for potentially involved pro- and antiapoptotic proteins affecting the caspase-9 to caspase-3 progression are currently underway. HT-29 colon cancer cells and BT474 breast cancer cells were conspicuously insensitive to compounds **1a** and **6**, which might have to do with the

overexpression of the cellular apoptosis susceptibility (CAS) gene in these cell lines.[19] CAS functions in the mitotic spindle checkpoint and its overexpression was shown to correlate with tumor progression rather than apoptosis.[20] Nonmalignant fibroblasts were far less prone to apoptosis induced by even high concentrations of **1a** or **6a** as ascertained by the absence of the typical apoptotic features. This tolerance of fibroblasts when compared to cancer cells is a pharmacologically interesting aspect.

Experimental Section

Chemistry. (2*E*)-3-[4′-Methoxy-3′-(tetrahydropyranyloxypropyl)]phenyl-1-(3′,4′,5′-trimethoxyphenyl)prop-2-en-1-one (2a). Typical Procedure. Anhydrous K_2CO_3 (922 mg, 6.76 mmol) was added to a stirring solution of chalcone **1a**[2] (222 mg, 0.65 mmol) in dry DMF (10 mL) whereupon the color of the solution turned red. After 10 min 3-tetrahydropyranyloxypropyl 1-bromide (1.44 g, 6.46 mmol) and TBAI (50 mg) were added and the reaction mixture was stirred under argon at room temperature for 24 h. It was diluted with ethyl acetate and brine, the water phase was extracted twice with ethyl acetate, and the combined organic phases were washed with brine, dried over Na_2SO_4, filtered, and concentrated in vacuum. The oily residue was purified by column chromatography on silica gel 60 to leave **2a** as a yellow oil (300 mg, 0.62 mmol, 95%): R_f = 0.43 (hexane/ethyl acetate 1:1).

(2*E*)-3-[4′-Methoxy-3′-(3′′-hydroxypropyl)]phenyl-1-(3′,4′,5′-trimethoxyphenyl)prop-2-en-1-one (3a). Typical Procedure. THP ether **2a** (300 mg, 0.62 mmol) was dissolved in ethanol (50 mL), PPTS (100 mg) was added, and the resulting mixture was stirred under reflux for 1 h. The solvent was evaporated, the oily residue thus obtained was taken up in ethyl acetate, washed once with water, dried, filtered, concentrated in vacuum, and purified by column chromatography (hexane/ethyl acetate 1:2), leaving the product as a yellow oil (210 mg, 0.52 mmol, 84%) which solidified upon standing: mp 116 °C; R_f = 0.26.

(*E*)-3-(4′-Methoxyphenyl)-1-(3′,4′,5′-trimethoxyphenyl)-prop-2-en-1-one-3′-yl 6-(*tert*-butoxy-carbonylaminomethyl)nicotinate (4a). Typical Procedure. 6-(*tert*-Butoxycarbonylaminomethyl)nicotinic acid[8] (140 mg, 0.56 mmol) was dissolved in dry DMF (2 mL) and treated with Et_3N (90 μL, 0.65 mmol) and 2,4,6-trichlorobenzoyl chloride (100 μL, 0.65 mmol). The resulting suspension was stirred under argon at room temperature for 20 min. A solution of chalcone **1a** (190 mg, 0.55 mmol) and DMAP (138 mg, 1.12 mmol) in dry DMF/toluene (1:9, 10 mL) was added, and the resulting mixture was stirred under argon at room temperature for 16 h. After dilution with ethyl acetate and washing with water the organic phase was dried over Na_2SO_4 and concentrated in vacuum. The residue was purified by column chromatography on silica gel 60 (hexane/ethyl acetate 1:1) to leave **4a** as a yellow oil (220 mg, 0.38 mmol, 68%): R_f = 0.25.

(*E*)-2-Methoxy-5-[3′-oxo-3′-(3′′,4′′,5′′-trimethoxyphenyl)-prop-1′-enyl]phenyl 6-aminomethylnicotinate bis(hydrochloride) (5a). Typical Procedure. Compound **4a** (210 mg, 0.36 mmol) was treated with 4 M HCl/dioxane (10 mL) at room temperature for 1 h. The formed precipitate was collected, washed with diethyl ether, dried, and used as such for the next step. Yield, 166 mg (0.30 mmol, 83%); light-brown solid of mp 165 °C.

***cis*-{(*E*)-2-Methoxy-5-[3′-oxo-3′-(3′′,4′′,5′′-trimethoxyphenyl) prop-1′-enyl]phenyl 6-aminomethylnicotinate}dichloridoplatinum(II) (6a). Typical Procedure.** Ligand **5a** (160 mg, 0.29 mmol) was dissolved in THF (5 mL) and treated with an aqueous solution of K_2PtCl_4 (121 mg, 0.29 mmol). The resulting colorless precipitate was redissolved by addition of THF. The pH value was adjusted to 5−6 with aqueous NaOH, and the reaction mixture was stirred at room temperature for 24 h. The formed precipitate was collected, washed in turn with water and diethyl ether, and finally dried in vacuum. Yield, 166 mg (0.22 mmol, 77%) of **6a**; yellow solid of mp >250 °C (dec).

Biological Studies. 1. Cytotoxicity Assays. Cell Lines and Culture Conditions. Twenty-one cell lines from nine entities (summarized in Table 1) were used for the evaluation of the cytotoxicity of the chalcones. Most of them were obtained from the American Type Culture Collection (ATCC), Rockville, MD, and from the German National Resource Center for Biological Material (DSMZ), Braunschweig, Germany. Cell lines were maintained as monolayer cultures in RPMI 1640 supplemented with 10% heat inactivated fetal bovine serum (Biochrom KG Seromed, Germany) and streptomycin/penicillin (GIBCO, Germany). Cultures were grown at 37 °C in a humidified atmosphere of 5% CO_2/95% air.

SRB Assay and Regrowth Analyses. Dose−response curves of the cell lines exposed to drug concentrations of 0.001−10 μM were established using the sulforhodamine-B (SRB) microculture colorimetric assay[21] and performed as previously described.[22] Briefly, cells were seeded into 96-well plates on day 0 at cell densities previously determined to ensure exponential cell growth during the period of the experiment. On day 1, cells were treated with the respective concentration range of the drugs, and the percentage of surviving cells relative to untreated controls was determined on day 5. For analysis of tumor cell regrowth after drug treatment, the SRB assay as decribed above was extended. After 96 h of exposure to the serial dilutions of drugs the cells were either fixed (day 0 after treatment) or washed drug-free and grown in fresh media for additional spells of time (2, 4, 6, 10 days). Appropriate concentrations were chosen to unveil differences in regrowth kinetics.

2. Immunoblotting. With Caspase-9 Antibodies. HL-60 cells (0.5×10^6 cells/mL) were incubated (37 °C, 5% CO_2, 95% humidity) with 10 μM test compound (in 1% DMF/99% PBS) for up to 30 h. At specified time intervals 2 mL aliquots were withdrawn. The cells were centrifuged and suspended in 100 μL of lysis buffer [50 mM Tris-HCl, 150 mM NaCl, 1% Triton X-100, 2% protease inhibitor cocktail Set III (Calbiochem), pH 7.4], vortexed, and incubated on ice for 15 min.[23] The proteins were separated on a 12% SDS−PAGE using 60 μg of protein per pocket[24] and blotted on a PVDF membrane. The membrane was then blocked by treatment with 10% milk powder in AP-T (0.1 M Tris-HCl, 0.1 M NaCl, 0.25 mM $MgCl_2$, 1% Tween-20, pH 7.4) for 1 h, washed three times for 10 min with AP-T, and finally incubated with the primary antibody (Calbiochem, 1:10.000 in AP-T). After another three washing steps the secondary antibody conjugated with horseradish-peroxidase (Calbiochem, 1:10.000 in AP-T) was applied. After another three washing steps visualization was conducted using Roti-Lumin (Roth) and Amersham Hyperfilm ECL (GE Healthcare). The film was exposed for 10 min.

With Antibodies for Caspase-3, PARP, and Actin. Cells were harvested, rinsed twice with PBS, and lysed in RIPA buffer [50 mM Tris-HCl, pH 8.0, 150 mM NaCl, 1% NP40, 0.5% DOC, 0.1% SDS] supplemented with a protease inhibitor cocktail (Sigma). Insoluble components were removed by centrifugation, and protein concentrations were measured (BIO-RAD protein assay, Bio-Rad, Germany). After boiling for 5 min in SDS-loading buffer (62.5 mM Tris-HCl, pH 6.8, 20% glycerol, 2% SDS, 100 mM DTT) 40 μg of protein per lane was separated by SDS−PAGE and electroblotted onto nitrocellulose membrane (Bio-Rad). Equal protein loadings were ensured by Ponceau S staining (Sigma). Membranes were blocked with 5% milk powder in PBST for 1 h and probed for 2 h with the following antibodies diluted in PBST/5% milk: actin (C-2) mouse monoclonal (0.5 μg/mL) (Santa Cruz Biotechnology), caspase-3 (Clon 33) mouse monoclonal (0.5 μg/mL) (MBL Biozol), PARP mouse monoclonal (4C10-5) (BD Pharmingen). Immunocomplexes were visualized by enhanced chemiluminescence (Amersham Pharmacia Biotech, U.K.) using horseradish peroxidase-conjugated antimouse or antirabbit IgG (Santa Cruz Biotechnology).

3. Colorimetric Caspase-3 Assays. These assays were performed in accordance with the manufacturer's recommendations using the CASPASE-3 cellular activity assay kit PLUS (Biomol, Plymouth Meeting, PA). This employs *N*-acetyl-Asp-Glu-Val-Asp-*p*-nitroaniline (Ac-DEVD-*p*NA) as a substrate for caspase-3 enzyme

with or without inhibitor Ac-DEVD-CHO added. Briefly, HL-60 cells were treated with test compound **1a** or **6a** for the indicated periods of time, harvested, and then lysed with the buffer provided in the kit (supplemented with 0.1% Triton X-100). The cleavage of the substrate DEVD bonded to the chromophore *p*-nitroanilide (*p*NA) was measured by reading the absorbance (at 405 nm wavelength) of the samples (maintained at 37 °C) at 15 min increments for 90 min. The rate of cleavage of *p*NA [(pmol/min)/μg of protein] was calculated from the initial slope of the absorbance vs time curves.

4. Tubulin Polymerization Assay. Analysis of tubulin polymerization was performed with a tubulin polymerization assay kit (Cytoskeleton) according to the manufacturer's instructions. The assay is fluorescence-based, and tubulin polymerization was monitored by measuring RFU (relative fluorescence units) on a SpectraFluorPlus (Tecan, Switzerland) using the following filters: excitation 360 nm, emission 465 nm.

Acknowledgment. This work was supported by a grant from the Deutsche Forschungsgemeinschaft (Grant Scho 402/8-2). We are indebted to Franziska Reipsch for technical assistance and to Dr. Florenz Sasse from the Helmholtz Center for Infection Research, Braunschweig (Germany), for additional tubulin binding experiments.

Supporting Information Available: Purity data for new compounds, spectroscopic data of compounds **2a**, **3a**, **4a**, **5a**, **6a**, syntheses and characterization of derivatives **2b**, **3b**, **4b**, **4c**, **5b**, **5c**, **6b**, **6c**, an experimental description of the TUNEL assay, and various experiments on the interactions of **1a** and **6** with DNA. This material is available free of charge via the Internet at http://pubs.acs.org.

References

(1) Tron, G. C.; Pirali, T.; Sorba, G.; Pagliai, F.; Busacca, S.; Genazzani, A. A. Medicinal chemistry of combretastatin A4: present and future directions. *J. Med. Chem.* **2006**, *49*, 3033–3044.

(2) Ducki, S.; Forrest, R.; Hadfield, J. A.; Kendall, A.; Lawrence, N. J.; McGown, A. T.; Rennison, D. Potent antimitotic and cell growth inhibitory properties of substituted chalcones. *Bioorg. Med. Chem. Lett.* **1998**, *8*, 1051–1056.

(3) Stoll, R.; Renner, C.; Hansen, S.; Palme, S.; Klein, C.; Belling, A.; Zeslawski, W.; Kamionka, M.; Rehm, T.; Mühlhahn, P.; Schumacher, R.; Hesse, F.; Kaluza, B.; Voelter, W.; Engh, R. A.; Holak, T. A. Chalcone derivatives antagonize interactions between the human oncoprotein MDM2 and p53. *Biochemistry* **2001**, *40*, 336–344.

(4) Cabrera, M.; Simoens, M.; Falchi, G.; Lavaggi, M. L.; Piro, O. E.; Castellano, E. E.; Vidal, A.; Azqueta, A.; Monge, A.; de Cerain, A. L.; Sagrera, G.; Seoane, G.; Cerecetto, H.; Gonzalez, M. Synthetic chalcones, flavanones, and flavones as antitumoral agents: biological evaluation and structure−activity relationships. *Bioorg. Med. Chem.* **2007**, *15*, 3356–3367.

(5) Meng, C. Q.; Ni, L.; Worsencroft, K. J.; Ye, Z.; Weingarten, M. D.; Simpson, J. E.; Skudlarek, J. W.; Marino, E. M.; Suen, K.-L.; Kunsch, C.; Souder, A.; Howard, R. B.; Sundell, C. L.; Wasserman, M. A.; Sikorski, J. A. Carboxylated, heteroaryl-substituted chalcones as inhibitors of vascular cell adhesion molecule-1 expression for use in chronic inflammatory diseases. *J. Med. Chem.* **2007**, *50*, 1304–1315.

(6) Vogel, S.; Ohmayer, S.; Brunner, G.; Heilmann, J. Natural and non-natural prenylated chalcones: synthesis, cytotoxicity and anti-oxidative activity. *Bioorg. Med. Chem.* **2008**, *16*, 4286–4293.

(7) Kamal, A.; Shankaraiah, N.; Prabhakar, S.; Reddy, C. R.; Markandeya, N.; Reddy, K. L.; Devaiah, V. Solid-phase synthesis of new pyrrolobenzodiazepine−chalcone conjugates: DNA-binding affnity and anticancer activity. *Bioorg. Med. Chem. Lett.* **2008**, *18*, 2434−2439.

(8) Schobert, R.; Biersack, B. *cis*-Dichloroplatinum(II) complexes with aminomethylnicotinate and -isonicotinate ligands. *Inorg. Chim. Acta* **2005**, *358*, 3369–3376.

(9) Inanaga, J.; Hirata, K.; Saeki, H.; Katsuki, T.; Yamaguchi, M. A rapid esterification by means of mixed anhydride and its application to large-ring lactonization. *Bull. Chem. Soc. Jpn.* **1979**, *52*, 1989–1993.

(10) Schobert, R.; Biersack, B.; Dietrich, A.; Grotemeier, A.; Müller, T.; Kalinowski, B.; Knauer, S.; Voigt, W.; Paschke, R. Monoterpenes as drug shuttles: cytotoxic (6-aminomethylnicotinate) dichloridoplatinum(II) complexes with potential to overcome cisplatin resistance. *J. Med. Chem.* **2007**, *50*, 1288–1293.

(11) Schobert, R.; Bernhardt, G.; Biersack, B.; Bollwein, S.; Fallahi, M.; Grotemeier, A.; Hammond, G. L. Steroid conjugates of dichloro(6-aminomethylnicotinate)platinum(II): effects on DNA, sex hormone binding globulin, the estrogen receptor, and various breast cancer cell lines. *ChemMedChem* **2007**, *2*, 333–342.

(12) Coggiola, B.; Pagliai, F.; Allegrone, G.; Genazzani, A. A.; Tron, G. C. Synthesis and biological activity of mustard derivatives of combretastatins. *Bioorg. Med. Chem. Lett.* **2005**, *15*, 3551–3554.

(13) Gavrieli, Y.; Sherman, Y.; Ben-Sasson, S. A. Identification of programmed cell death in situ via specific labeling of nuclear DNA fragmentation. *J. Cell Biol.* **1992**, *119* (3), 493–501.

(14) Psahoulia, F. H.; Drosopoulos, K. G.; Doubravska, L.; Andera, L.; Pintzas, A. Quercetin enhances TRAIL-mediated apoptosis in colon cancer cells by inducing the accumulation of death receptors in lipid rafts. *Mol. Cancer Ther.* **2007**, *6*, 2591–2599.

(15) Shankar, S.; Chen, Q.; Siddiqui, I.; Sarva, K.; Srivastava, R. K. Sensitization of TRAIL-resistant LNCaP cells by resveratrol: molecular mechanism and therapeutic potential. *J. Mol. Signaling* **2007**, *2*, 7.

(16) Shankar, S.; Chen, Q.; Sarva, K.; Siddiqui, I.; Srivastava, R. K. Curcumin enhances the apoptosis-inducing potential of TRAIL in prostate cancer cells: molecular mechanism of apoptosis, migration and angiogenesis. *J. Mol. Signaling* **2007**, *2*, 10.

(17) Shin, S.; Sung, B. J.; Cho, Y. S.; Kim, H. J.; Ha, N. C.; Hwang, J. I.; Chung, C. W.; Jung, Y. K.; Oh, B. H. An antiapoptotic protein human survivin is a direct inhibitor of caspase-3 and -7. *Biochemistry* **2001**, *40*, 1117–1123.

(18) Asselin, E.; Mills, G. B.; Tsang, B. K. XIAP regulates Akt activity and caspase-3-dependent cleavage during cisplatin-induced apoptosis in human ovarian epithelial cancer cells. *Cancer Res.* **2001**, *61*, 1862–1868.

(19) Brinkmann, U.; Gallo, M.; Polymeropoulos, M. H.; Pastan, I. The human CAS (cellular apoptosis susceptibility) gene mapping on chromosome 20q13 is amplified in BT474 breast cancer cells and part of aberrant chromosomes in breast and colon cancer cell lines. *Genome Res.* **1996**, *6*, 187–194.

(20) Behrens, P.; Brinkmann, U.; Wellmann, A. CSE1L/CAS: its role in proliferation and apoptosis. *Apoptosis* **2003**, *8*, 39–44.

(21) Papazisis, K. T.; Geromichalos, G. D.; Dimitriadis, K. A.; Kortsaris, A. H. Optimization of the sulforhodamine B colorimetric assay. *J. Immunol. Methods* **1997**, *208*, 151–158.

(22) Müller, T.; Voigt, W.; Simon, H.; Frühauf, A.; Bulankin, A.; Grothey, A.; Schmoll, H.-J. Failure of activation of caspase-9 induces a higher threshold for apoptosis and cisplatin resistance in testicular cancer. *Cancer Res.* **2003**, *63*, 513–521.

(23) Wagner, S.; Hafner, C; Allwardt, D; Jasinska, J.; Ferrone, S.; Zielinski, C. C.; Scheiner, O.; Wiedermann, U.; Pehamberger, H.; Breitender, H. Vaccination with a human high molecular weight melanoma-associated antigen mimotope induces a humoral response inhibiting melanoma cell growth in vitro. *J. Immunol* **2005**, *174*, 976–982.

(24) Laemmli, U. K. Cleavage of structural proteins during the assembly of the head of bacteriophage T4. *Nature* **1970**, *227*, 680–685.

JM801001D